

Universal supercritical current distributions in 3D random resistor networks

Feng Shi, Simi Wang, Peter J. Mucha, and M. Gregory Forest*

*Department of Mathematics and
Institute for Advanced Materials, Nanoscience and Technology,
University of North Carolina at Chapel Hill, Chapel Hill, NC 27599*

Inspired by percolation-induced properties of nano-particle composites [Nan *et al.*, Annu. Rev. Mater. Res. 40, 131 (2010)], and in particular the robust electrical property gains at and above percolation threshold, we revisit the classical setting of percolation in random resistor networks. We simulate and analyze scaling behaviors of the percolation-induced distribution of currents in the network, first confirming the celebrated power-law distribution of small currents. We further identify a robust exponential distribution in the large current tail that persists above but close to threshold, whereas the power-law scaling in the small currents does not.

Motivated by questions about macroscopic electronic properties in material science, we consider the classic problem of bond percolation [1, 2] in a three-dimensional $L \times L \times L$ cubic lattice and the state of currents conducting through the percolating bonds. In the seminal work of De Arcangelis *et al.* [3, 4], a hierarchical lattice model is given for the percolating backbone of the network, which yields a log-normal current distribution in the network; this model was later generalized by Lin *et al.* [5]. These models capture many features of the network such as the multifractal behavior of the current distribution (i.e., an infinite hierarchy of exponents is needed to describe the moments of the distribution). However, they failed to predict the power law distribution of small currents (Straley [6] and Duering *et al.* [7, 8]). Even more importantly, the previous models do not appear to adequately capture the distribution of bond currents that dominate measurable behavior.

Current distributions have fundamental importance in material science. Low moments of the current distribution dictate physically measurable properties, e.g., the second moment describes the bulk conductance [3, 9], so that measurable scaling behavior at or above percolation threshold (cf. [10]) is inherited from the current distribution. Another illustration is in the study of breakdown of random media [11–14]. This critical network property motivated studies on the size and location of the largest current in the network [15–17]. We note the maximum current does not inform properties of the large current distribution. Here we analyze the entire current distribution, reproducing previous results about small currents while revealing scaling behaviors of the large current tail of the distribution that controls bulk response above percolation threshold.

Each edge of the lattice takes conductance 1 with probability p , (we call such a conducting edge a bond and p is the bond density), and conductance 0 with probability $1-p$. We seek to understand the relationship between the electrical and topological properties of the resulting bond percolation network. In order to model an externally-driven bulk electrical response, we consider two perfectly conducting $L \times L$ plates to be present at opposite ends

of the cube, representing the sink and source of current (in response to either an external voltage drop or current source).

For each realization of the random resistor network model, a breadth-first search algorithm [18] is applied to find the union of percolating clusters that connect the two plates. The 2-core of this union is identified, with forced inclusion of the two plates, because only these bonds can carry nonzero currents under the defined electrical problem. Near the percolation threshold, the number of relevant bonds in the system is reduced by almost 90% by this preprocessing. More importantly, we observe improved numerical precision by this *a priori* elimination of many of the zero-current bonds. The Kirchhoff law [19] is then solved on these percolating 2-cores with a standard linear solver, giving the current on each bond. A statistical description of the network properties is obtained by averaging over many realizations (typically 1000 realizations for each bond density and system size).

The bond percolation threshold p_c for an infinite 3D cubic lattice is $p_c \doteq 0.2488$ [20]. For $p < p_c$, no percolating cluster forms (with measurable probability) and thus current does not pass through the network. For convenience, let $f(i)$ be the probability density function (PDF) of the current magnitudes across the population of current-carrying bonds (that is, ignoring zero-current bonds where present). Let $h(x)$ be the corresponding PDF (again, restricted to non-zero currents) of the logarithmic current $X = \ln(I)$. The two distributions are related by $h(x) = f(e^x)e^x$.

The logarithmic current distribution $h(x)$ and current distribution $f(i)$ near ($p = 0.25$) and above ($p = 0.29$) the threshold are shown in Figure 1 for a unit voltage source. First, the logarithmic transformation of current exposes the small current region; the left panel in Figure 1 shows that the small currents obey a power-law distribution up to a peak in the current distribution, agreeing with Straley [6] and Duering *et al.* [7, 8]. Second, for relatively large currents (i.e., to the right of the peak of the $h(x)$ distribution), Figure 1 (right) suggests exponential $f(i)$ distributions. This general shape of the current distribution persists as bond density p increases near and

above threshold. The implications are two-fold: there is an exponential large current tail at and above percolation, whereas the small current tail disintegrates above the critical bond density. We are cautious to rule out finite size effects since the $p = 0.25$ system size is comparable to the correlation length [1]. Specifically, near threshold, the correlation length ξ scales as $\xi \propto (p - p_c)^{-0.9}$ [1], which we will include in our study below.

While the small-current behavior is well understood and the maximum current has been studied extensively, little is known about the large current tail of the distribution even though the large currents dominate bulk properties. E.g., the second moment of the current distribution determines the bulk conductance. We focus here on the large current tail, revealing a robust exponential distribution above but close to percolation threshold. The empirical densities of the current for a unit voltage source near percolation threshold ($p = 0.25$) and above threshold ($p = 0.29$) for different system sizes are shown in Figure 2 and Figure 3 respectively. Despite slightly larger noise at bond density $p = 0.25$, the straight lines in both figures point to exponential tails of the current distributions, and the rate of the exponential decay increases with the system size L . In order to meaningfully capture an externally-imposed voltage drop in the thermodynamic limit ($L \rightarrow \infty$), and to better understand the effect of system size on the current distribution, we carry out a finite-size scaling analysis on the distributions. Let $f_L(i)$ be the probability density function (PDF) of the current at system size L for a unit voltage source; then by properly rescaling $f_L(i)$ with L , we aim to eliminate the effect of the system size:

$$L^{-u} f_L(L^{-v} i) = f^\infty(i), \quad (1)$$

where $f^\infty(i)$ is a function independent of L , and u and v are critical exponents to be determined. By tuning u and v , we confirm that the densities for different system sizes collapse onto a single curve with $u = 1$ and $v = 1$ (see the insets of Figure 2 and Figure 3). This is the expected result for a material with bulk conductance: the total resistance per unit cross-sectional area increases $\sim L$. In other words, $f^\infty(i)$ is the limiting current distribution for system size L and external voltage source $V^* = L$ (made dimensionless by the definition of bonds as unit conductances). Therefore in a finite system the current density for a unit voltage source scales as:

$$f_L(i) = L f^\infty(Li). \quad (2)$$

Note that equation (2) requires that any multifractal property of the overall current distribution comes from the small current tail, since the k^{th} moment M_k of the large currents described by this finite-size scaling is a simple scaling function of L . Specifically,

$$M_k = \int_0^\infty i^k f_L(i) di = \int_0^\infty i^k L f^\infty(Li) di \propto L^{-k}. \quad (3)$$

To confirm this simple scaling form of the moments, we compute the first several sample moments at bond density 0.25 for varying system sizes and plot them in Figure 4. The sample moments are calculated as $\hat{M}_k = \frac{1}{N} \sum_b i_b^k$, where N is the number of bonds with nonzero current and the sum of bond currents i_b is taken over all current-carrying bonds, b . The scaling forms of the moments are not exactly the same as Equation (3) due to the multifractal property of small currents; however for large moments the exponential tail of the current distribution becomes dominant and thus the scaling relationship approaches Equation (3).

To confirm the universal nature of the exponential tail in the large values of the current distribution, we now focus on a unit current source flowing between the two plates. Current distributions for a unit voltage source differ from those for a unit current source by a factor of the bulk conductance C , because of the linearity of the system. Formally, denoting the density of the current distribution for the unit current source by $g_L(i)$, the density $f_L(i)$ of the current distribution for a unit voltage source can be written as: $f_L(i) = g_L(i/C)/C$. Then assuming $g_L(i) \sim e^{-\lambda i}$ for large currents yields

$$f_L(i) \sim \exp - \frac{\lambda i}{C}, \quad (4)$$

for large currents. Therefore, the rate of the exponential tail of $f_L(i)$ being independent of the bond density (over an observed range) indicates a linear relationship between the rate of decay of the exponential tail of $g_L(i)$ and the bulk conductance, and vice versa.

It would seem surprising for these two properties to scale linearly with one another. To quantify this relationship, exponential distributions are fitted to the current distributions for a unit current source at various bond densities and their rates are plotted against the bond densities in Figure 5, along with the scaling behavior of the bulk conductance. These results indicate that the rate of the exponential decay $\lambda(p)$ and the bulk conductance $C(p)$ have similar scaling behaviors with respect to bond density near and above the percolation threshold, which can be deduced from the figure:

$$\lambda(p) \propto (p - p_c)^{1.969 \pm 0.077}, \quad (5)$$

$$C(p) \propto (p - p_c)^{1.911 \pm 0.012}. \quad (6)$$

Both the underlying exponential distribution and the power-law scalings become invalid further from the threshold as the system saturates. We notice their clear breakdown at $p = 0.35$ and beyond (as indicated in the supplemental materials [21]).

Finally we superimpose all the limiting current distributions $f^\infty(i) = L^{-1} f_L(L^{-1} i)$ for a wide range of system sizes L and bond densities p in Figure 6, with colors representing the ratio $L/(p - p_c)^{-0.9}$ as an indicator of the extent to which our result is affected by the finite size ef-

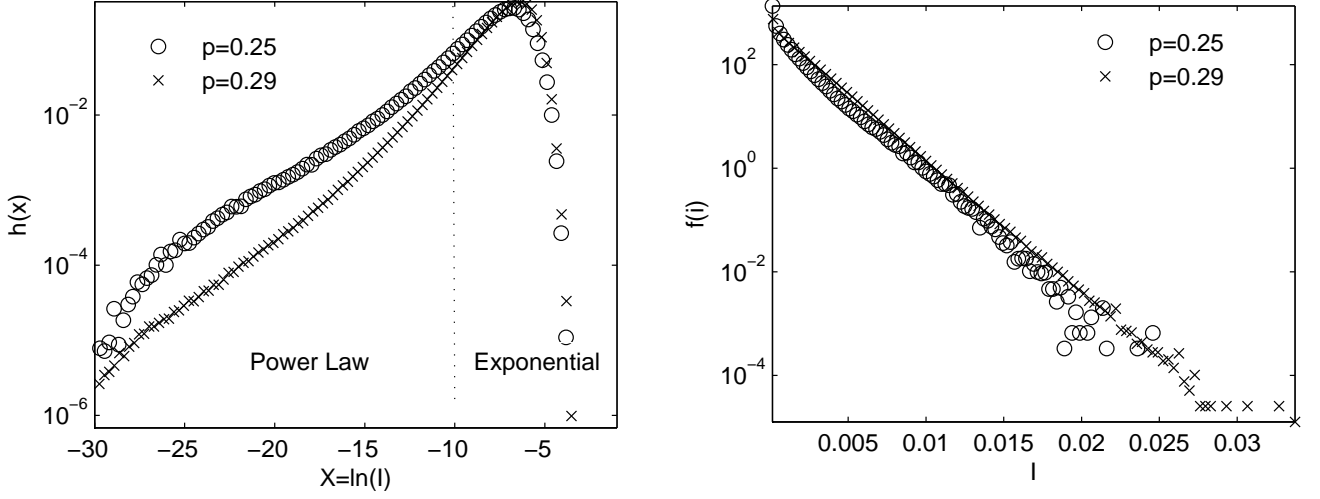


FIG. 1. Distribution $h(x)$ of the logarithmic current (left) and distribution $f(i)$ of the current (right) near threshold ($p = 0.25$) and above threshold ($p = 0.29$) in $100 \times 100 \times 100$ random resistor networks.

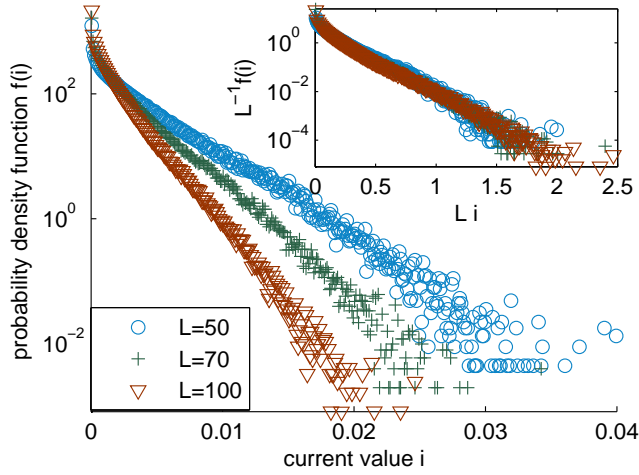


FIG. 2. (Color online) Empirical probability density function of the current in an $L \times L \times L$ cubic lattice at bond density 0.25 (which we note is quite close to the percolation threshold 0.2488) for various system sizes L . A constant unit voltage is imposed across the system. The plot is an average of 1000 realizations. The inset shows the same distributions rescaled by the system L with critical exponents $u = 1$ and $v = 1$.

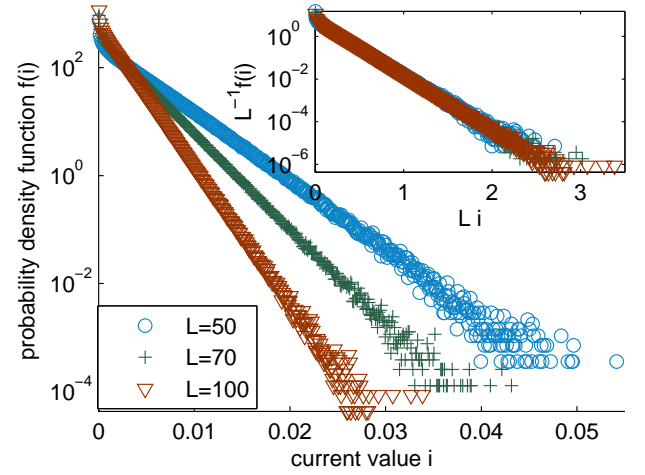


FIG. 3. (Color online) Empirical probability density function of the current in an $L \times L \times L$ cubic lattice at bond density 0.29 (which is above the percolation threshold 0.2488) for various system sizes L . A constant unit voltage is imposed across the system. The plot is an average of 1000 realizations. The inset shows the same distributions rescaled by the system L with critical exponents $u = 1$ and $v = 1$.

fect. Despite the noise at low system-size-to-correlation-length ratios, Figure 6 demonstrates apparent convergence to a universal class of exponential distributions for the large currents both near and above threshold. The rate of the exponential tail does not depend on the bond density and the simple scaling form of the tail of the current distribution with the system size remains the same. Again this universality of current distributions only holds close to threshold. Far above threshold the current distribution approaches a delta function which is the current

distribution at $p = 1$ where every bond on the paths perpendicular to the two plates carries the same amount of current while all other bonds carry zero current. Again, we notice significant difference in the current distributions starting at approximately $p = 0.35$ (as indicated in the supplemental materials [21]).

Recall that the second moment of the current distribution is related to the conductance of the network. Specifi-

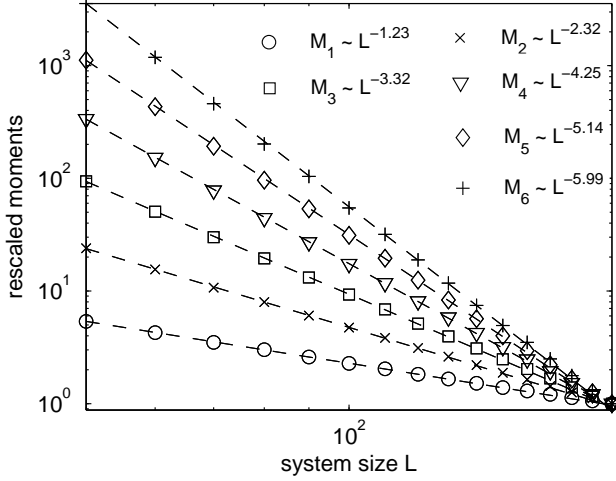


FIG. 4. Scaling of the first 6 sample moments with respect to the system size L . The bond density is fixed at $p = 0.25$ and the system size L varies from 50 to 200. The fitted equations of the moments M_k are shown in the figure (cf. Equation (3)). Curves are normalized by their values at $L = 200$.

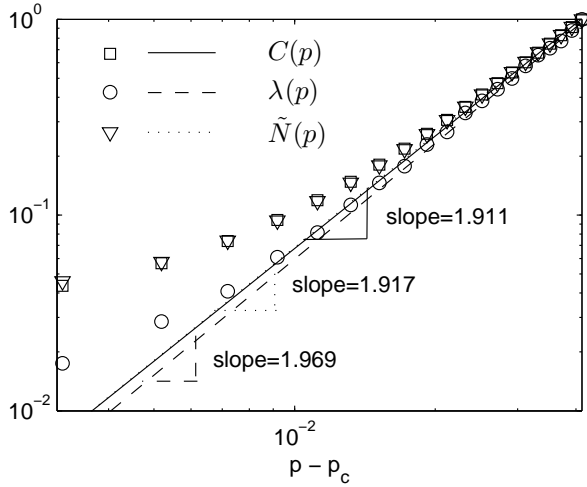


FIG. 5. Scaling behaviors against bond density $p - p_c$ for, the bulk conductance ($C(p)$), the rate of the exponential tail of the current distribution ($\lambda(p)$), and the number of bonds with current larger than 10^{-3} ($\tilde{N}(p)$). The system size is fixed at $L = 100$ and the bond density p varies from 0.25 to 0.29. Curves are normalized by their values at $p = 0.29$.

cally, due to the conservation of the energy in the system,

$$\frac{V^2}{R} = \sum_b i_b^2 r_b, \quad (7)$$

where V and R are the external voltage and the bulk resistance of the system respectively, i_b is the value of the current on a bond, $r_b = 1$ is the resistance of a bond, and the sum is taken over all bonds with nonzero current. For a unit external voltage source, Equation (7) can be

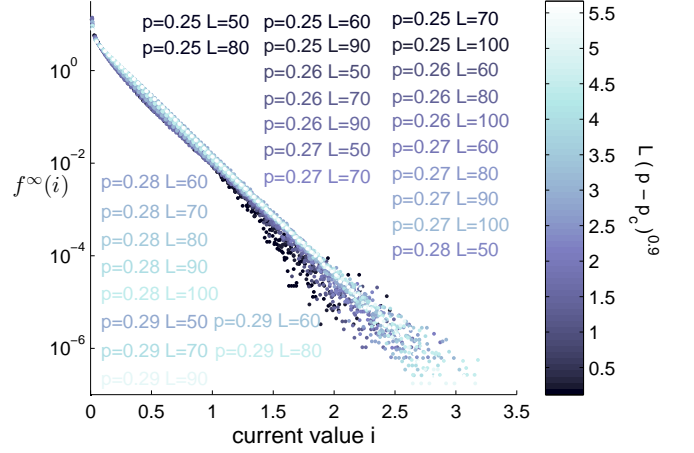


FIG. 6. (Color Online) Limiting current distributions $f^\infty(i) = L^{-1}f_L(L^{-1}i)$ at different system sizes and bond densities. Colors represent the ratio $L/(p-p_c)^{-0.9}$ as an indicator of the system size relative to the correlation length.

rewritten as $C = R^{-1} = \sum_b i_b^2$, where C is the bulk conductance of the network. Dividing by the number of current-carrying bonds N , we recover the conductance from the continuous current distribution:

$$\frac{C}{N} = \frac{\sum i_b^2}{N} = \int_0^\infty i^2 f_L(i) di. \quad (8)$$

Equation (8) connects the scaling behavior of the bulk conductance to that of the current distribution. Since the second moment of the current distribution $f_L(i)$ is dominated by the exponential tail of $f_L(i)$ which is shown to be independent of the bond density p , the number of bonds carrying large currents (whose magnitudes are assumed to be larger than 10^{-3}) $\tilde{N}(p)$ and the bulk conductance $C(p)$ have the same scaling form with respect to the bond density p . The scaling of $\tilde{N}(p)$ with respect to p is shown in Figure 5, and the corresponding scaling form is:

$$\tilde{N}(p) = (p - p_c)^{1.917 \pm 0.013}. \quad (9)$$

The balance of Equation (8) conditioned on large currents implies that there is an intrinsic consistency between the power-law scaling of the conductance and the exponential tail of the current distribution.

In conclusion, we have identified a robust and universal exponential distribution which persists above but close to threshold, describing the large current tail of the current distribution for the response of a cubic bond percolation network to an external field. In the supercritical regime above the percolation threshold, it is precisely this range of currents that is most relevant for describing and diagnosing the macroscopic electrical response for materials applications.

-
- * Email: forest@unc.edu; Mailing Address: CB 3250, UNC Chapel Hill, Chapel Hill, NC 27599-3250; Phone: (919) 962-9606
- [1] D. Stauffer and A. Aharony, *Introduction to percolation theory* (CRC Press, 1994).
 - [2] G. Deutscher, R. Zallen, and J. Adler, *Percolation structures and processes* (A. Hilger, 1983).
 - [3] L. De Arcangelis, S. Redner, and A. Coniglio, *Physical Review B* **31**, 4725 (1985).
 - [4] L. de Arcangelis, S. Redner, and A. Coniglio, *Physical Review B* **34**, 4656 (1986).
 - [5] B. Lin, Z.-Z. Zhang, and B. Hu, *Physical Review A* **44**, 960 (1991).
 - [6] J. P. Straley, *Physical Review B* **39**, 4531 (1989).
 - [7] E. Duering and D. J. Bergman, *Journal of Statistical Physics* **60**, 363 (1990).
 - [8] E. Duering, R. Blumenfeld, D. J. Bergman, A. Aharony, and M. Murat, *Journal of Statistical Physics* **67**, 113 (1992).
 - [9] R. Rammal, C. Tannous, P. Breton, and A. M. S. Tremblay, *Physical Review Letters* **54**, 1718 (1985).
 - [10] C.-W. Nan, Y. Shen, and J. Ma, *Annual Review of Materials Research* **40**, 131 (2010).
 - [11] L. de Arcangelis, S. Redner, and H. Herrmann, *Journal de Physique Lettres* **46**, 585 (1985).
 - [12] P. M. Duxbury, P. L. Leath, and P. D. Beale, *Physical Review B* **36**, 367 (1987).
 - [13] B. Kahng, G. Batrouni, S. Redner, L. de Arcangelis, and H. Herrmann, *Physical Review B* **37**, 7625 (1988).
 - [14] G. G. Batrouni and A. Hansen, *Physical Review Letters* **80**, 325 (1998).
 - [15] B. Kahng, G. Batrouni, and S. Redner, *Journal of Physics A: Mathematical and General* **20**, L827 (1987).
 - [16] J. Machta and R. A. Guyer, *Physical Review B* **36**, 2142 (1987).
 - [17] Y. S. Li and P. M. Duxbury, *Physical Review B* **36**, 5411 (1987).
 - [18] D. E. Knuth, *Art of Computer Programming, Volume 1: Fundamental Algorithms*, 3rd ed. (Addison-Wesley Professional, 1997).
 - [19] G. Strang, *Introduction to Applied Mathematics* (Wellesley-Cambridge Press, 1986).
 - [20] C. D. Lorenz and R. M. Ziff, *Physical Review E* **57**, 230 (1998).
 - [21] “See supplemental materials at [url will be inserted by publisher] for numeric results at bond densities far from threshold.”.